

Escape Criteria And Fractal Dynamics Of Hyperbolic Cosine Functions Via Picard–Thakur Iteration

Babawuro Z¹., Manjak N. H¹., Kwami A. M¹., Adamu M. Y¹., And Ismaila O. I.

¹Department Of Mathematics, Abubakar Tafawa Balewa University Bauchi, Nigeria.

²Department Of Mathematics, University Of Maiduguri, Nigeria.

Abstract

Fractals are mathematical structures that repeat themselves at multiple scales with applications in modeling natural and physical phenomena. Many authors have explored Julia and Mandelbrot sets derived from polynomial and standard transcendental functions such as sine, cosine, exponential, and logarithmic functions. However, little attention has been given to hyperbolic functions, despite their rich mathematical elegant. The concept of escape criteria, is a fundamental principle use to determine whether a variable in the complex plane belongs to the set or not and majority of fractals dynamical behavior are determined by escape criteria, which utilize various iterative procedures. In this work, we explore stunning new fractals of Julia and Mandelbrot sets of complex transcendental hyperbolic cosine function by establishing the escape radii using the Picard–Thakur iteration, which is a four-step extension of the classical Picard scheme. Python algorithms are used to generate Julia and Mandelbrot sets across varying parameter choices. Results reveal that the power index r strongly influences boundary density, while the coefficients determine symmetry and structural distortions. Real parameters yield symmetric fractals, whereas complex values produce twisted and irregular geometries. Iteration weights and control parameters α, β, γ further refine complexity, color, and computational speed. Compared to earlier fractals generated from sine, cosine, exponential, and logarithmic functions, the hyperbolic cosine sets display higher density and richer structures. This demonstrates the effectiveness of the Picard–Thakur scheme in expanding the mathematical framework for fractal generation.

Keywords: Julia set, Mandelbrot set, Picard–Thakur iteration, escape criterion, and fractals.

Date of Submission: 25-01-2026

Date of Acceptance: 05-02-2026

I. Introduction

Fractal structures are found mostly in the natural phenomena, where their shapes repeat at smaller and smaller scales, and make them look very complex. Typical examples can be seen in Trees, clouds, and mountains that display a moderate degree of fractal behavior. The visibility of these patterns, range from microscopic to large scale global features (Taylor, 2021). Human eyes easily adjust to these repeating patterns through what is called the fractal fluency model. Because of this, a Science Design Lab (SDL) was set up to create such patterns, mainly to study how they affect people in relation to the environment (Smith et al 2020). Fractal patterns were applied in the design of relaxation floors to promote the positive effects of natural geometry. These open spaces allow people to experience a pleasant natural environment. Since 2019 the designs have won ten human centered awards (Tasaddiq et al, 2024). Fractals are produced by using iterative processes where certain equations or rules are applied finitely many times. Mandelbrot pointed out that certain objects are difficult to measure with standard methods because their roughness remains the same at different scales. This property, known as fractal dimension, allows scientists to describe and model irregular shapes across various fields (Mandelbrot, 1975). Fractals do not only give visual images of these shapes, but they also help in carrying out accurate calculations for modeling and analysis (Rani & Kumar, 2004).

Novel escape criterion for hyperbolic sine and cosine functions have been developed using three-step fixed point iteration method With Python algorithms, Julia and Mandelbrot sets were generated under the new criteria and visually appealing fractal structures. With the parameters $q = 4$ and $q = 8$ it significantly influenced fractal forms, producing high color intensity and circular pattern (Sahan & Atalan, 2025). Recent work has applied the escape criterion for creating fractals via Picard Thakur hybrid iteration scheme, a four-step method with faster convergence than other popular iterative techniques, to establish new escape criteria for fractal generation. Using these criteria, three algorithms were developed and employed to generate well-known fractal classes of Julia sets, Mandelbrot sets, and multicorns. The study considered the complex polynomial function $\mathfrak{D}(z) = z^m + b$ where $m \geq 2, b \in C$ and analysed how variations in parameters affects fractal structures and image generation time. The

result obtained shows that even small changes in parameter values, significantly altered fractal patterns and increasing these parameters from 0 to 1 drastically reduced computation time (Tasaddiq et al, 2024).

Building on previous progress the fractal dynamical behaviors of the hyperbolic cosine function are determined via a new four step escape criterion of Picard–Thakur iteration scheme, this criterion is applied to generate visually appealing Julia and Mandelbrot fractals which can be valuable for understanding its dynamics and a basis for creating fractal art in fashion design, image compression, antenna design e.t.c [Kharbanda & Bajaj (2013), Cohen (1997), Fisher (1994)].

Definition 1. (Julia set) The set of all point which has a bounded orbit under f is refer to as filled-in Julian set of f and is denoted by B_λ .

Mathematically,

$$B_\lambda = \{z : |f_\lambda^n(z)| \neq \infty \text{ as } n \rightarrow \infty\}.$$

The boundary of the filled-in Julian set denoted by J_λ is called Julian set of f .

Definition 2 (Mandelbrot set) The Mandelbrot set M of some complex map $f_\lambda(z)$, Where $\lambda \in \mathbb{C}$, is the set of values of the complex parameter λ which, $f_\lambda^n(z) \neq \infty$, as $n \rightarrow \infty$.

Mathematically:

$$M = \{\lambda : \lambda \in \mathbb{C}, \lim_{n \rightarrow \infty} f_\lambda^n(z) \neq \infty \text{ as } n \rightarrow \infty\}.$$

Definition 3. The Picard Orbit Consider f to be a non-empty set and $f : C \rightarrow C$. Picard's orbit for any initial point $z_0 \in C$ can be defined as the set of all iterates of z_0 , denoted as

$$O(f, z_0) = \{z_n : z_n = f(z_{n-1}), n = 1, 2, 3, \dots\}. \text{ (Devany 1992).}$$

Definition 4. Picard–Thakur orbits iteration procedure: Let C be a subset of complex numbers, and $f_c : C \rightarrow C$ is a mapping. For the initial point $z_0 \in C$, the Picard Thakur orbit is defined as

$$z_{n+1} = f_c(x_n)$$

$$x_n = (1 - \alpha_1)f_c(\lambda_n) + \alpha_1 f_c(y_n)$$

$$y_n = (1 - \beta_1)\lambda_n + \beta_1 f_c(\lambda_n)$$

$$\lambda_n = (1 - \gamma_1)z_n + \gamma_1 f_c(z_n)$$

Where $\alpha_1, \beta_1, \gamma_1 \in (0, 1)$.

The above sequence of iterates given by the Equation above is known as the Picard–Thakur orbit, which can be written as PTO $(f_c, z_n, \alpha_1, \beta_1, \gamma_1)$.

II. Escape Criteria For Complex Cosh Functions

The escape criterion performs an essential role in generating and analyzing Julia sets as well as Mandelbrot sets and their variants. We develop the following escape criteria for the complex valued Cosh functions to explore and compare the new mutants of Julia and Mandelbrot sets via Picard Thakur iteration method.

Let $T_c(z) = a \cosh(z^r) + bz + c$

Since,

$$|\cosh(z^r)| = \left| \sum_{m=0}^{\infty} \frac{z^{r(2m)}}{2m!} \right|$$

$$= \left| 1 + \frac{z^{2r}}{2!} + \frac{z^{4r}}{4!} + \dots \right|$$

$$\begin{aligned} &> \left| \frac{z^{2r}}{2!} + \frac{z^{4r}}{4!} + \dots \right| \\ &= \left| z^r \left| \frac{z^r}{2!} + \frac{z^{3r}}{4!} + \dots \right| \right| \\ &\geq |z^r| |\lambda_1| \end{aligned}$$

$$\text{Where } |\lambda_1| \in (0,1] \text{ and } |\lambda_1| \leq \left| \frac{z^r}{2!} + \frac{z^{3r}}{4!} + \dots \right| = \left| \sum_{m=1}^{\infty} \frac{z^{r(2m-1)}}{(2m)!} \right|$$

Similarly

$$\begin{aligned} |\cosh(\lambda^r)| &\geq |\lambda^r| |\lambda_2|, \text{ where } |\lambda_2| \in (0,1] \text{ and } |\lambda_2| \leq \left| \sum_{m=1}^{\infty} \frac{z^{r(2m-1)}}{(2m)!} \right| \\ |\cosh(y^r)| &\geq |y^r| |\lambda_3|, \text{ where } |\lambda_3| \in (0,1] \text{ and } |\lambda_3| \leq \left| \sum_{m=1}^{\infty} \frac{z^{r(2m-1)}}{(2m)!} \right| \\ |\cosh(x^r)| &\geq |x^r| |\lambda_4|, \text{ where } |\lambda_4| \in (0,1] \text{ and } |\lambda_4| \leq \left| \sum_{m=1}^{\infty} \frac{z^{r(2m-1)}}{(2m)!} \right| \end{aligned}$$

Theorem 1

Let $f_c(z) = a \cosh(z^r) + bz + c$ be a complex transcendental Cosh function and

$$|z| \geq |c| > \text{Max} \left\{ \left(\frac{2+|b|}{\gamma_1 |a| |\lambda_1|} \right)^{\frac{1}{r-1}}, \left(\frac{2+|b|}{\beta_1 |a| |\lambda_2|} \right)^{\frac{1}{r-1}}, \left(\frac{2+|b|}{|a| (|\alpha_1| |\lambda_3| - |\lambda_2|)} \right)^{\frac{1}{r-1}}, \left(\frac{2+|b|}{|a| |\lambda_4|} \right)^{\frac{1}{r-1}} \right\},$$

Where $0 < \alpha_1, \beta_1, \lambda_1 < 1$ and $c \in C$.

Define

$$z_{n+1} = f_c(x_n) \quad (1a)$$

$$x_n = (1 - \alpha_1) f_c(\lambda_n) + \alpha_1 f_c(y_n) \quad (1b)$$

$$y_n = (1 - \beta_1) \lambda_n + \beta_1 f_c(\lambda_n) \quad (1c)$$

$$\lambda_n = (1 - \gamma_1) z_n + \gamma_1 f_c(z_n) \quad (1d)$$

Then $|z_n| \rightarrow \infty$ as $n \rightarrow \infty$

Proof: for $f_c(z) = a \cosh(z^r) + bz + c$ and $n = 0$,

$$|\lambda_n| = |(1 - \gamma_1) z_n + \gamma_1 f_c(z_n)| \quad (1d)$$

$$= |(1 - \gamma_1) z_n + \gamma_1 f_c(z_n)|$$

$$= |(1 - \gamma_1) z_n + \gamma_1 (a \cosh(z^r) + bz + c)|$$

$$\geq |\gamma_1 (a \cosh(z^r) + bz) + (1 - \gamma_1) z_n| - |\gamma_1 c|$$

$$\geq \gamma_1 |a| |\cosh(z^r)| - \gamma_1 |b| |z| - |z_n| + \gamma_1 |z| - \gamma_1 |c|$$

Now, by using $|z| \geq |c|$, we have

$$|\lambda| \geq \gamma_1 |a| |z^r| |\lambda_1| - \gamma_1 |b| |z| - |z|$$

$$\geq \gamma_1 |a| |z^r| |\lambda_1| - |b| |z| - |z|$$

$$= |z|(\gamma_1|a|z^{r-1}|\lambda_1| - |b| - 1).$$

since $|z| > \left(\frac{2+|b|}{\gamma_1|a|\lambda_1} \right)^{\frac{1}{r-1}}$ implies that $\gamma_1|a|z^{r-1}|\lambda_1| > 2+|b|$, so $\gamma_1|a|z^{r-1}|\lambda_1| - |b| - 1 > 1$.

Therefore, $|\lambda| > |z|$ (2)

Now, in the second step we have

$$|y| = |(1-\beta_1)\lambda_n + \beta_1 f_c(\lambda_n)| (1c)$$

$$\begin{aligned} &= |(1-\beta_1)\lambda_n + \beta_1(a \cosh(\lambda^r) + b\lambda + c)| \\ &\geq |\beta_1(a \cosh(\lambda^r) + b\lambda) + (1-\beta_1)\lambda| - |\beta_1 c| \\ &\geq |\beta_1(a \cosh(\lambda^r) + b\lambda)| - (1-\beta_1)|\lambda| - |\beta_1 c| \\ &\geq \beta_1|a|\lambda^r - |\lambda_2| - \beta_1|b|\lambda - |\lambda| + \beta_1|\lambda| - \beta_1|c| \end{aligned}$$

By using $|\lambda| > |z|$ we obtain

$$\begin{aligned} |y| &\geq \beta_1|a|z^r|\lambda_2| - \beta_1|b|z - |z| \\ &\geq \beta_1|a|z^r|\lambda_2| - |b|z - |z| \\ &= |z|(\beta_1|a|z^{r-1}|\lambda_2| - |b| - 1). \end{aligned}$$

since $|z| > \left(\frac{2+|b|}{\beta_1|a|\lambda_2} \right)^{\frac{1}{r-1}}$ implies that $\beta_1|a|z^{r-1}|\lambda_2| > 2+|b|$, so $\beta_1|a|z^{r-1}|\lambda_2| - |b| - 1 > 1$.

Therefore, $|y| > |z|$. (3)

In third step we have

$$\begin{aligned} |x_n| &= |(1-\alpha_1)f_c(\lambda_n) + \alpha_1 f_c(y_n)| (1b) \\ &= |(1-\alpha_1)(a \cosh(\lambda^r) + b\lambda + c) + \alpha_1(a \cosh(y^r) + by + c)| \\ &\geq \alpha_1|a \cosh(y^r) + by| - \alpha_1|c| - (1-\alpha_1)|a \cosh(\lambda^r) + b\lambda| - (1-\alpha_1)|c| \\ &\geq \alpha_1|a|\cosh(y^r) - \alpha_1|b|y - \alpha_1|c| - (1-\alpha_1)|a|\cosh(\lambda^r) - (1-\alpha_1)|b|\lambda - (1-\alpha_1)|c| \\ &\geq \alpha_1|a|\cosh(y^r) - \alpha_1|b|y - \alpha_1|c| - |a|\cosh(\lambda^r) + \alpha_1|a|\cosh(\lambda^r) - |b|\lambda + \alpha_1|b|\lambda - |c| + \alpha_1|c| \end{aligned}$$

By neglecting $\alpha_1|a|\cosh(\lambda^r)$ and using (2), (3) and $|z| \geq |c|$, we obtain

$$\begin{aligned} |x| &\geq \alpha_1|a|z^r|\lambda_3| - \alpha_1|b|z - \alpha_1|z| - |a|z^r|\lambda_2| - |b|z + \alpha_1|b|z - |z| + \alpha_1|z| \\ &= \alpha_1|a|z^r|\lambda_3| - |a|z^r|\lambda_2| - |b|z - |z| \\ &= |z|(\alpha_1|a|z^{r-1}|\lambda_3| - |a|z^{r-1}|\lambda_2| - |b| - 1). \end{aligned}$$

Since $|z| > \left(\frac{2+|b|}{|a|(\alpha_1|\lambda_3| - |\lambda_2|)} \right)^{\frac{1}{r-1}}$ implies that $|z|^{r-1}|a|(\alpha_1|\lambda_3| - |\lambda_2|) > 2+|b|$, so

$$\alpha_1|a|z^{r-1}|\lambda_3| - |a|z^{r-1}|\lambda_2| - |b| - 1 > 1.$$

Therefore $|x| > |z|$.

Now, in the last step, which is from (1a) for $z_{n+1} = f_c(x_n)$, we have

$$\begin{aligned} |z_1| &= |f_c(x_n)| \\ &= |a \cosh(x^r) + bx + c| \\ &\geq |a \cosh(x^r) + bx| - |c| \\ &\geq |a| |u^r| |\lambda_4| - |b| |u| - |c| \\ &\geq |a| |z^r| |\lambda_4| - |b| |u| - |c| \\ &\geq |z| (|a| |z^{r-1}| |\lambda_4| - |b| - 1). \end{aligned}$$

When applying similar arguments repeatedly, we obtain

$$\begin{aligned} |z_2| &\geq |z| (|a| |z^{r-1}| |\lambda_4| - |b| - 1)^2 \\ |z_3| &\geq |z| (|a| |z^{r-1}| |\lambda_4| - |b| - 1)^3 \\ &\dots \\ |z_n| &\geq |z| (|a| |z^{r-1}| |\lambda_4| - |b| - 1)^n \end{aligned}$$

Since $|z| > \left(\frac{2+|b|}{|a|\lambda_4} \right)^{\frac{1}{r-1}}$ implies that $|a| |z^{r-1}| |\lambda_4| > 2+|b|$ and $|a| |z^{r-1}| |\lambda_4| - |b| - 1 > 1$, hence we have

$$|z_n| \rightarrow \infty \text{ as } n \rightarrow \infty.$$

Corollary1: Assume that $|z_j| > \max \left\{ |c|, \left(\frac{2+|b|}{\gamma_1|a|\lambda_1} \right)^{\frac{1}{r-1}}, \left(\frac{2+|b|}{\beta_1|a|\lambda_2} \right)^{\frac{1}{r-1}}, \left(\frac{2+|b|}{|a|(\alpha_1|\lambda_3| - |\lambda_2|)} \right)^{\frac{1}{r-1}}, \left(\frac{2+|b|}{|a|\lambda_4} \right)^{\frac{1}{r-1}} \right\}$. Then $|z_{j+1}| \geq (1 + \lambda_1)^k |z_j|$ and $|z_{j+1}| \rightarrow \infty$ as $k \rightarrow \infty$.

III. Algorithms:

In this section, attractive fractal patterns were produced for complex hyperbolic cosine functions using the Picard–Thakur iteration scheme (1a-1d). The algorithms were written in Python 3.12 to generate the Julia and Mandelbrot sets.

Algorithm 1 The Julia set
Setup:
Take a complex number $c = u + iv$. Initialize the variables $\alpha_1, \beta_1, \gamma_1, \lambda_1, \lambda_2, \lambda_3, \lambda_4, a, b$ Consider first iteration $z_0 = x + iy$.
Iterate:
$\begin{aligned} z_{n+1} &= f_c(x_n); \\ x_n &= (1 - \alpha_1)f_c(\lambda_n) + \alpha_1 f_c(y_n); \\ y_n &= (1 - \beta_1)\lambda_n + \beta_1 f_c(\lambda_n); \\ \lambda_n &= (1 - \gamma_1)z_n + \gamma_1 f_c(z_n); n \geq 0, \end{aligned}$
Where $f_c(z) = a \cosh(z^r) + bz + c$ $r = 2, 3, 4, \dots, 0 < \alpha_1, \beta_1, \gamma_1 < 1, 0 < \lambda_1, \lambda_2, \lambda_3, \lambda_4 \leq 1$.
Stop:
$ z_n > \text{Escape radius} = \max \left\{ c , \left(\frac{2+ b }{\gamma_1 a \lambda_1} \right)^{\frac{1}{r-1}}, \left(\frac{2+ b }{\beta_1 a \lambda_2} \right)^{\frac{1}{r-1}}, \left(\frac{2+ b }{ a (\alpha_1 \lambda_3 - \lambda_2)} \right)^{\frac{1}{r-1}}, \left(\frac{2+ b }{ a \lambda_4} \right)^{\frac{1}{r-1}} \right\}$
Count:
The number of iterations undertaken to escape.
Color:
Assign a color to each point based on the number of iterations needed to escape.

Algorithm 2 The Mandelbrot set
Setup:
Take a complex number $c = u + iv$.
Initialize the variables $\alpha_1, \beta_1, \gamma_1, \lambda_1, \lambda_2, \lambda_3, \lambda_4, a, b$
Consider first iteration $z_0 = c$.
Iterate:
$z_{n+1} = f_c(x_n);$
$x_n = (1 - \alpha_1)f_c(\lambda_n) + \alpha_1 f_c(y_n);$
$y_n = (1 - \beta_1)\lambda_n + \beta_1 f_c(\lambda_n);$
$\lambda_n = (1 - \gamma_1)z_n + \gamma_1 f_c(z_n); n \geq 0,$
Where $f_c(z) = a \cosh(z^r) + bz + c$ $r = 2, 3, 4, \dots, 0 < \alpha_1, \beta_1, \gamma_1 < 1, 0 < \lambda_1, \lambda_2, \lambda_3, \lambda_4 \leq 1$
Stop: $ z_n > \text{Escape radius} = \max \left\{ c , \left(\frac{2+ b }{\gamma_1 a \lambda_1 } \right)^{\frac{1}{r-1}}, \left(\frac{2+ b }{\beta_1 a \lambda_2 } \right)^{\frac{1}{r-1}}, \left(\frac{2+ b }{ a (\alpha_1\lambda_3 - \lambda_2)} \right)^{\frac{1}{r-1}}, \left(\frac{2+ b }{ a \lambda_4 } \right)^{\frac{1}{r-1}} \right\}.$
Count:
The number of iterations undertaken to escape.
Color:
Assign a color to each point based on the number of iterations needed to escape.

Mandelbrot sets for $f_c(z) = a \cosh(z^r) + bz + c$.

In this part of the study, we used the escape-time method to create the Mandelbrot set with a hyperbolic cosine-based function. The process was carried out for up to 10 iterations, depending on the values of the parameters. The steps for generating the Mandelbrot set are given in Algorithm 2.

Case1: For the function $f_c(z) = a \cosh(z^r) + bz + c$. Different sets of parameters, which are listed in **Table 1**.

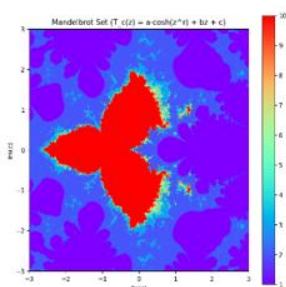


Figure 1i

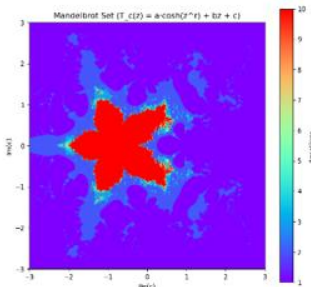


Figure 1ii

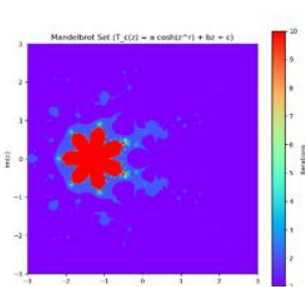


Figure 1iii

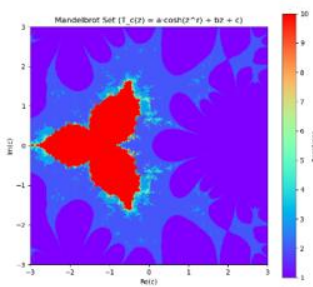


Figure 1iv

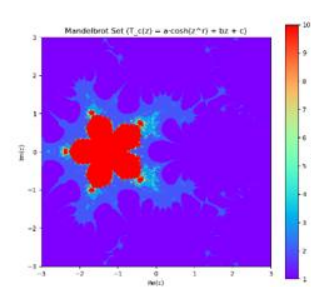


Figure 1v

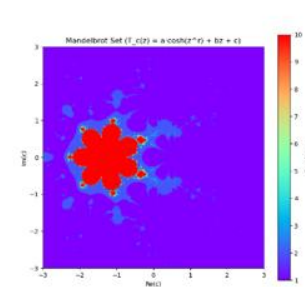


Figure 1vi

Table 1.

Figures	a	b	r	α_1	β_1	γ_1	λ_1	λ_2	λ_3	λ_4
Figure 1i	0.8000	0.2000	2	0.5000	0.5000	0.5000	0.8000	0.5000	0.7000	0.7000
Figure 1ii	0.8000	0.2000	3	0.5000	0.5000	0.5000	0.8000	0.5000	0.7000	0.7000
Figure 1iii	0.8000	0.2000	4	0.5000	0.5000	0.5000	0.8000	0.5000	0.7000	0.7000
Figure 1iv	0.4+0.9	0.6-0.2	2	0.7000	0.5000	0.3000	0.2000	0.3000	0.4000	0.5000
Figure 1v	0.4+0.9	0.6-0.2	3	0.7000	0.5000	0.3000	0.2000	0.3000	0.4000	0.5000

Figure 1vi 0.4+0.9 0.6-0.2 4 0.7000 0.5000 0.3000 0.2000 0.3000 0.4000 0.5000

Using the Picard Thakur iteration, we examined the influence of parameter variation on the structural patterns of Mandelbrot sets associated with the cosine hyperbolic function, with real values of a and b . For these values, the fractals produced showed gradual variation in complexity as the power r increased. This effect is clearly visible in Figures 1*i* – 1*vi*, where higher values of r produce denser and more intricate structures compared to lower values. The images illustrate how increasing r transforms the fractal structure. At lower values of r , the sets are simpler, while larger values of r produce richer boundary details and more compact patterns. This demonstrates that the power parameter r strongly influences the density and shape of Mandelbrot sets.

Case (2): When complex values are assigned to the parameters a and b , the quadratic Mandelbrot set, as shown in Figures 2

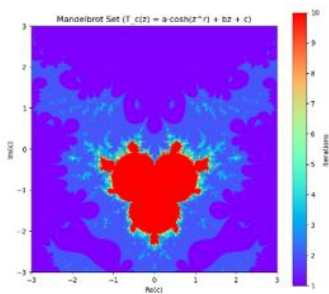


Figure 2i

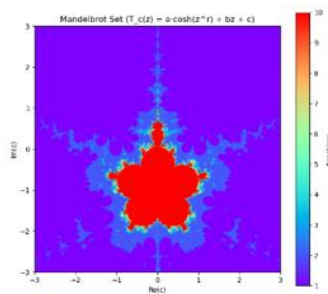


Figure 2ii

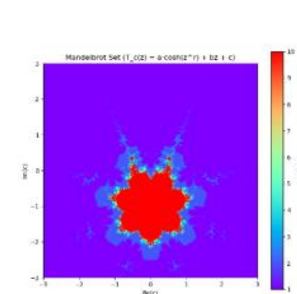


Figure 2iii

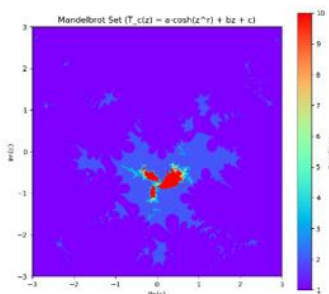


Figure 2iv

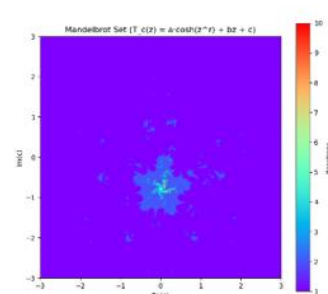


Figure 2v

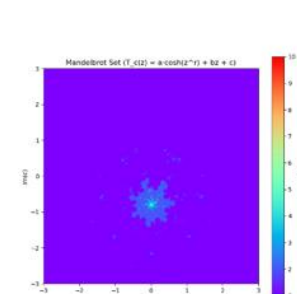


Figure 2vi

Table 2.

Figures	a	b	r	α_1	β_1	γ_1	λ_1	λ_2	λ_3	λ_4
Figure 2i	1.000i	0.0001i	2	0.6000	0.7000	0.8500	0.8000	0.5000	0.7000	0.7000
Figure 2ii	1.000i	0.0001i	3	0.6000	0.7000	0.8500	0.8000	0.5000	0.7000	0.7000
Figure 2iii	1.000i	0.0001i	4	0.6000	0.7000	0.8500	0.8000	0.5000	0.7000	0.7000
Figure 2iv	0.0+0.8i	1.2+0.4i	2	0.9000	0.9000	0.9000	0.0001	0.0001	0.0001	0.0001
Figure 2v	0.0+0.8i	1.2+0.4i	3	0.9000	0.9000	0.9000	0.0001	0.0001	0.0001	0.0001
Figure 2vi	0.0+0.8i	1.2+0.4i	4	0.9000	0.9000	0.9000	0.0001	0.0001	0.0001	0.0001

Parameter settings for Mandelbrot sets when a and b are complex. Using these values, the generated fractals resembled quadratic Mandelbrot structures, differing from those produced with real parameters. Figures 2*i* – 2*vi* show smoother transitions at the boundaries and more quadratic like forms. Complex parameter choices result in fractals that exhibit more irregularity and variation, indicating the strong effect of imaginary components in the iteration process.

Julia set for $f_c(z) = a \cosh(z^r) + bz + c$

We used the Picard–Thakur method to see how changing different parameters changes the look of Julia sets for our cosine function.

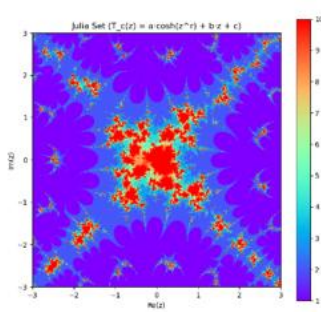


Figure 3i

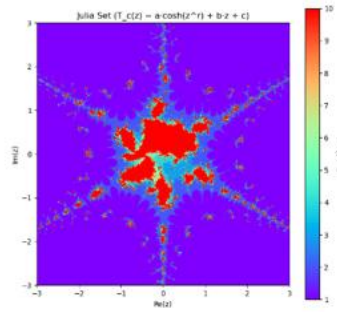


Figure 3ii

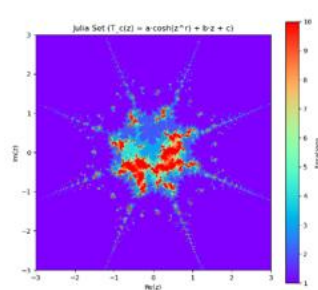


figure 3iii

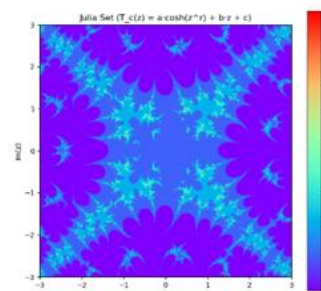


Figure 3iv

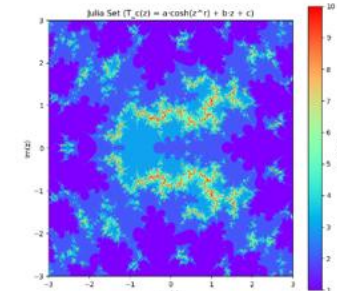


Figure 3v

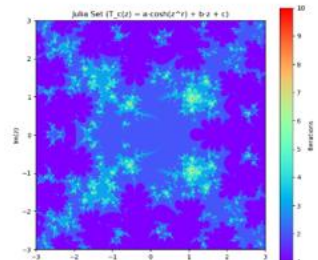


Figure 3vi

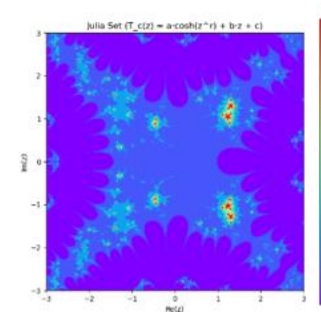


Figure 3vii

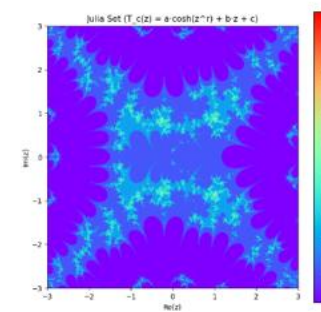


Figure 3viii

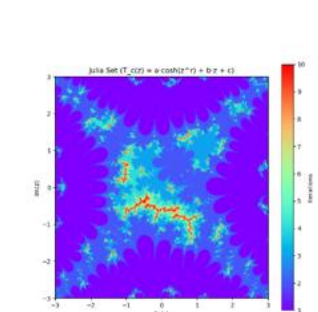


Figure 3ix

Table 3

Figures	a	b	c	r	α_1	β_1	γ_1	λ_1	λ_2	λ_3	λ_4
Figure 3i	1.2	0.2	-0.4+05j	2	0.009	0.009	0.008	0.006	0.007	0.008	0.009
Figure 3ii	1.2	0.2	-0.4+05j	3	0.009	0.009	0.008	0.006	0.007	0.008	0.009
Figure 3iii	1.2	0.2	-0.4+05j	4	0.009	0.009	0.008	0.006	0.007	0.008	0.009
Figure 3iv	1.2	0.2	0.003	2	0.009	0.009	0.008	0.006	0.007	0.008	0.009
Figure 3v	0.80	0.80	0.0075	2	0.5000	0.1000	0.0070	0.002	0.003	0.004	0.005
Figure 3vi	0.80	0.80	-0.0781+0.6694	2	1.500	0.100	0.007	0.002	0.003	0.004	0.005
Figure 3vii	0.80	0.80	0.3509+0.6194	2	0.002	0.002	0.002	0.752	0.753	0.754	0.755
Figure 3viii	0.80	0.80	0.3509	2	0.002	0.002	0.002	0.752	0.753	0.754	0.755
Figure 3ix	0.80	0.80	-0.3509i	2	0.002	0.002	0.002	0.752	0.753	0.754	0.755

Table 3 figure 3i – iii contains the constants a, b, c and iteration weights α, β, γ used for Julia set generation. These parameters significantly influence fractal patterns, often producing drastically different outcomes with only small changes. The Julia sets exhibit a variety of structures, from symmetric and self-similar forms to chaotic irregularities. Some sets display strong symmetry across the x axis, while others are asymmetric and highly complex. The color intensity is more pronounced when iteration weights increase, particularly for certain values of r , demonstrating the sensitivity of Julia sets to parameter variations.

IV. Conclusion

The research successfully developed escape criteria for hyperbolic cosine functions using Picard–Thakur iteration, leading to the generation of novel Julia and Mandelbrot fractals. It was demonstrate that the exponent r and the coefficients a, b , significantly control fractal complexity, while iteration weights and parameters λ fine-tune the density and symmetric Nature of the fractals generally yield symmetric fractals, while complex values introduce twists and irregularity fractals. Compared with sine, cosine, exponential, and logarithmic based fractals, the hyperbolic cosine fractals display higher density, more compact structures, and distinctive boundary patterns. This confirms the potential of the Picard–Thakur method as an efficient framework for studying new families of transcendental fractals.

Reference

- [1]. Cohen, N. (1997). Fractal Antenna Applications In Wireless Telecommunications. In Professional Program Proceedings. Electronic Industries Forum Of New England (Pp. 43-49). IEEE.
- [2]. Fisher, Y. (1994). Fractal Image Compression. *Fractals*, 2(03), 347-361.
- [3]. Kharbanda, M., & Bajaj, N. (2013). An Exploration Of Fractal Art In Fashion Design. In 2013 International Conference On Communication And Signal Processing (Pp. 226-230). IEEE.
- [4]. Mandelbrot, B.B.(1975), *Les Objects Fractals: Forme, Hasard Et Dimension*; Flammarion: Paris, France, Volume 17.Mathematics Vol. 3, Issue 2, Page 93-97
- [5]. Qi, H., Tanveer, M., Nazeer, W., & Chu, Y. (2020). Fixed Point Results For Fractal Generation Of Complex Polynomials Involving Sine Function Via Non-Standard Iterations. *IEEE Access*, 8, 154301-154317.
- [6]. Rani, M., & Kumar, V. (2004). Superior Julia Set. *Research In Mathematical Education*, 8(4), 261-277
- [7]. Rani, M., & Kumar, V. (2004). Superior Julia Set. *Research In Mathematical Education*, 8(4), 279-291
- [8]. Şahan, T., & Atalan, Y. (2025). Novel Escape Criteria For Complex-Valued Hyperbolic Functions Through A Fixed Point Iteration Method.
- [9]. Smith, J., Rowland, C., Mosleh, S., Taylor, R., Lesjak, M., & Himes, J. (2020), Relaxing Floors: Fractal Fluency In The Built Environment. *Nonlinear Dynamics, Psychology And Life Science*, 24(1), 127-141.
- [10]. Tanveer, M., Nazeer, W., & Gdawiec, K. (2023). On The Mandelbrot Set Of $Z^p + \log C^t$ Via The Mann And Picard–Mann Iterations. *Mathematics And Computers In Simulation*, 209, 184-204.
- [11]. Tassaddiq, A. (2022). General Escape Criteria For The Generation Of Fractals In Extended Jungck–Noor Orbit. *Mathematics And Computers In Simulation*, 196, 1-14.
- [12]. Tassaddiq, A., Tanveer , M., Israr, K., Arshad, M., Shehzad, K. & Srivastava, R. (2023). Multicorn Sets Of $Z^k + C^m$ Via S-Iteration With H-Convexity. *Fractal And Fractional*, 6(6), 486.
- [13]. Tassaddiq, A., Tanveer, M., Azhar, M., Lakhani, F., Nazeer, W., & Afzal, Z. (2024). Escape Criterion For Generating Fractals Using Picard–Thakur Hybrid Iteration. *Alexandria Engineering Journal*, 100, 331-339.
- [14]. Taylor, R. P.(2021), The Potential Of Biophilic Fractal Designs To Promote Health And Performance: A review Of Experiments And Applications. *Sustainability*, 13(2), 823.
- [15]. Zou, C., Shahid, A. A., Tassaddiq, A., Khan, A., & Ahmad, M. (2020). Mandelbrot Sets And Julia Sets In Picard-Mann Orbit. *IEEE Access*, 8, 64411-64421.